

**Special Section:**

Water-Energy-Carbon Fluxes Over Terrestrial Water Surfaces

**Key Points:**

- Lake-atmosphere CO<sub>2</sub> exchange was estimated using four common methods
- CO<sub>2</sub> concentration gradient flux estimates agreed in direction and magnitude with floating chambers but disagreed with eddy covariance
- Inconsistencies among methods highlight the spatial and temporal assumptions underlying methods and the need to acknowledge uncertainty

**Correspondence to:**D. E. Reed,  
david.edwin.reed@gmail.com**Citation:**

Baldocchi, A. K., Reed, D. E., Loken, L. C., Stanley, E. H., Huerd, H., & Desai, A. R. (2020). Comparing spatial and temporal variation of lake-atmosphere carbon dioxide fluxes using multiple methods. *Journal of Geophysical Research: Biogeosciences*, 125, e2019JG005623. <https://doi.org/10.1029/2019JG005623>

Received 27 DEC 2019

Accepted 29 NOV 2020

Accepted article online 2 DEC 2020

**Author Contributions:****Conceptualization:** David E. Reed, Ankur R. Desai**Data curation:** Angela K. Baldocchi, David E. Reed, Luke C. Loken, Hayley Huerd, Ankur R. Desai**Formal analysis:** Angela K. Baldocchi, David E. Reed, Ankur R. Desai**Funding acquisition:** Emily H. Stanley, Ankur R. Desai**Methodology:** David E. Reed, Luke C. Loken, Emily H. Stanley, Hayley Huerd, Ankur R. Desai**Project administration:** Emily H. Stanley, Ankur R. Desai

(continued)

## Comparing Spatial and Temporal Variation of Lake-Atmosphere Carbon Dioxide Fluxes Using Multiple Methods

Angela K. Baldocchi<sup>1</sup>, David E. Reed<sup>1,2</sup> , Luke C. Loken<sup>3</sup> , Emily H. Stanley<sup>3</sup> , Hayley Huerd<sup>4</sup>, and Ankur R. Desai<sup>1</sup> 

<sup>1</sup>Department of Atmospheric and Oceanic Sciences, University of Wisconsin-Madison, Madison, WI, USA,<sup>2</sup>Environmental Science, University of Science and Arts of Oklahoma, Chickasha, OK, USA, <sup>3</sup>Center for Limnology, University of Wisconsin-Madison, Madison, WI, USA, <sup>4</sup>Department of Environmental Engineering, University of California Merced, Merced, CA, USA

**Abstract** Lakes emit globally significant amounts of carbon dioxide (CO<sub>2</sub>) to the atmosphere, but quantifying these rates for individual lakes is extremely challenging. The exchange of CO<sub>2</sub> across the air-water interface is driven by physical, chemical, and biological processes in both the lake and the atmosphere that vary at multiple spatial and temporal scales. None of the methods we use to estimate CO<sub>2</sub> flux fully capture this heterogeneous gas exchange. Here, we compared concurrent CO<sub>2</sub> flux estimates from a single lake based on commonly used methods. These include floating chambers (FCs), eddy covariance (EC), and two concentration gradient-based methods labeled fixed (F-*p*CO<sub>2</sub>) and spatial (S-*p*CO<sub>2</sub>). At the end of summer, cumulative carbon fluxes were similar between EC, F-*p*CO<sub>2</sub>, and S-*p*CO<sub>2</sub> methods (−4, −4, and −9.5 gC m<sup>−2</sup>), while methods diverged in directionality of fluxes during the fall turnover period (−50, 43, and 38 gC m<sup>−2</sup>). Collectively, these results highlight the discrepancies among methods and the need to acknowledge the uncertainty when using any of them to approximate this heterogeneous flux.

**Plain Language Summary** Lakes comprise a small percentage of the landscape, but they are active and complex areas of carbon cycling. Lakes receive mixed carbon inputs from upstream sources, process this carbon internally, store it in sediments and biomass, and export it downstream. In addition, some fraction of the carbon in lakes exchanges into and out of the atmosphere, linking lakes with the global atmosphere. The exchange of carbon dioxide across lake surfaces has globally significant implications, but quantifying these rates has yet to be fully resolved. Here, we compared four methods of estimating diffusive carbon dioxide exchange between the atmosphere and the lake surface. Flux rates generally agreed during the summer, but estimates diverged in the fall, a critical time period with elevated carbon cycling rates. These discrepancies among methods may arise because of the high degree of spatial and temporal variability in gas exchange and our limited ability to portray and scale these processes accurately. In the future, we need to improve both the resolution of observations and how we process those observations to better measure carbon gas exchange between lakes and the atmosphere.

### 1. Introduction

Lakes are a major component of the Earth's carbon cycle, and an increasing focus has been placed on carbon dynamics within inland waters (Biddanda, 2017; Tranvik et al., 2009; Williamson et al., 2009). A substantial fraction of the organic carbon that is delivered to or fixed within lakes is outgassed to the atmosphere as carbon dioxide (CO<sub>2</sub>) (Cole et al., 2007; Cory et al., 2014). While there is consensus that collectively lakes and other inland waters emit meaningful amounts of CO<sub>2</sub> to the atmosphere, it remains extremely difficult to calculate spatially and temporally resolved emission rates for individual lakes. This difficulty is because the exchange of CO<sub>2</sub> across the air-water interface is driven by multiple physical, chemical, and biological processes in both the lake and the atmosphere that vary at multiple spatial and temporal scales. The scientific community lacks methods to fully capture the spatial and temporal heterogeneity in gas exchange between lakes and the atmosphere. Thus, every estimate of global CO<sub>2</sub> emissions from lakes has uncertainty.

**Resources:** Luke C. Loken, Emily H. Stanley, Ankur R. Desai  
**Supervision:** David E. Reed, Luke C. Loken, Ankur R. Desai  
**Validation:** Ankur R. Desai  
**Visualization:** Angela K. Baldocchi, David E. Reed, Ankur R. Desai  
**Writing – original draft:** Angela K. Baldocchi, David E. Reed  
**Writing – review & editing:** Angela K. Baldocchi, David E. Reed, Luke C. Loken, Emily H. Stanley, Hayley Huerd, Ankur R. Desai

The reason that lake-atmosphere fluxes are difficult to quantify in part is because they vary in magnitude (Raymond et al., 2013), in time (Reed et al., 2018), and across space (Natchimuthu et al., 2016). In many temperate dimictic lakes, seasonal phenologies in ice cover and stratification govern the direction and magnitude of CO<sub>2</sub> flux. Large off-gassing events occur during periods of vertical mixing such as ice-off and fall turnover (Denfeld et al., 2016). Lakes with higher productivity show pronounced temporal variation in CO<sub>2</sub> flux (Maberly et al., 2012), characterized by influx during the summer periods coinciding with higher rates of primary production (Reed et al., 2018). Thus, for even a single lake, flux estimation needs to be continuous and year-round in order to capture the temporal heterogeneity in gas exchange. Spatially, heterogeneity in metabolic processes, hydrology, and turbulence can have pronounced impacts on CO<sub>2</sub> flux from the lake surface. Rivers flowing into lakes typically differ in a number of physical, chemical, and biological properties that can create contrasts in *p*CO<sub>2</sub> in habitats where they enter a lake (Chmiel et al., 2019). Further, spatial heterogeneity varies temporally (Loken, Stanley, et al., 2019; Natchimuthu et al., 2016) due to changes in river flow, lake mixing, and biological processes. Thus, to accurately measure CO<sub>2</sub> flux from a single lake, we need to incorporate both spatial and temporal variation.

Any calculations of lake-atmosphere CO<sub>2</sub> flux are limited in either spatial or temporal extent. Perhaps the simplest and most cost-effective method for measuring gas efflux from lakes is using floating chambers (FCs) (Bastviken et al., 2015). Chambers are placed atop the lake surface, and the flux is derived from the gas accumulation rate within the chamber. However, flux chambers characterize only a small area of the lake for what is typically a short deployment. Further, the chamber itself can alter turbulence, thus biasing gas exchange within the chamber environment (Vachon et al., 2010). Historically, FCs for CO<sub>2</sub> required manual gas sampling followed by laboratory determination of gas concentrations, while newer FCs integrate continuous CO<sub>2</sub> sensors and automatic purging mechanisms that allow for longer deployments (Bastviken et al., 2015; Jonsson et al., 2008; Martinsen et al., 2018). While a single measurement is small in its spatial scale, multiple chambers have been used to quantify the spatial variability of gas emissions within and among lake habitats (Natchimuthu et al., 2016; Tangen et al., 2016). Similarly, measuring temporal variability of fluxes using FCs is common but in both cases, characterizing spatial and/or temporal variability with this approach is time intensive. New automated chambers show promise in increasing the duration of continuous observation (Duc et al., 2012).

A common alternative to FCs is modeling exchange rates using the concentration gradient or boundary layer method (*F-p*CO<sub>2</sub>) (Cole & Caraco, 1998; MacIntyre et al., 2010; Read et al., 2012). The flux of any gas across the air-water interface is controlled at the molecular level (Kitaigorodskii & Donelan, 1984), and fluxes are estimated using differences between *p*CO<sub>2</sub> on opposing sides of the air-water boundary and an estimate of water turbulence or gas transfer velocity (*k*). Spatial scales of *p*CO<sub>2</sub> measurements within the water column are on the order of cubic centimeters and typically fixed in space. Estimation of *k* is typically based on empirically derived models using wind speed, lake size, and/or water density gradients (Crusius & Wanninkhof, 2003; MacIntyre et al., 2010; Read et al., 2012). The difficulty in modeling *k* stems from the fact that *k* changes in response to weather events and varies within lakes due to lake and environmental conditions (Natchimuthu et al., 2016; Vachon et al., 2013). Moreover, estimation of *k* can vary by multiple orders of magnitude simply due to model choice (Dugan et al., 2016). Recent *p*CO<sub>2</sub> studies have shown that scaling *k* from point measurements to the lake scale strongly underestimates emissions (Mammarella et al., 2015; Schubert et al., 2012). New methods have been developed to quickly quantify spatial variation in *p*CO<sub>2</sub> (Bastviken et al., 2015; Crawford et al., 2015) and have revealed substantial spatial variations in *p*CO<sub>2</sub> and fluxes within individual lakes and reservoirs (Loken, Crawford, et al., 2019; Natchimuthu et al., 2016; Paranaíba et al., 2018). Despite their flaws, boundary layer methods have provided the most frequent and comprehensive understanding of CO<sub>2</sub> exchange between lakes and the atmosphere (Balmer & Downing, 2011; Duarte et al., 2008; Raymond et al., 2013), yet most assume spatial homogeneity and are reliant on physical lake models that have large uncertainty.

A third approach for quantifying lake CO<sub>2</sub> fluxes is eddy covariance (EC) (Morin et al., 2018; Reed et al., 2018). In contrast to the water-based approaches, EC uses measurements of concentrations of gas in the atmosphere along with high-frequency measurements of wind speeds in three dimensions. While this top-down flux method seems like the silver bullet for quantifying CO<sub>2</sub> flux, EC has several assumptions built into estimation and is spatially limited. It relies on measurement during periods with air movement

sufficient to generate turbulent airflow with eddies and includes uncertainty of footprint models that estimate the area over which fluxes are being measured (i.e., the footprint), with a single flux estimate integrating over  $\sim 1 \text{ km}^2$ . Turbulence and footprint issues can lead to upward of 80% of EC data being excluded (Reed et al., 2018). EC estimates represent the average flux from a portion of the lake surface, which bias observations toward nearshore areas (Morin et al., 2018) where most towers are located. Despite these limitations, EC offers a promising method for assessing carbon fluxes from lakes (Vesala et al., 2012).

Because each technique for measuring carbon flux has its limitations, efforts have been made to compare these methods. However, these investigations have been limited to relatively short time periods (Erkkila et al., 2018; Podgrajsek et al., 2016; Schubert et al., 2012). These authors found discrepancies among methods for quantifying  $\text{CO}_2$  flux in both space and time. While estimates of carbon fluxes are critical for understanding the global carbon cycle, how best to measure lake-atmosphere fluxes remains challenging and is an open question for the scientific community.

In order to compare methods of quantifying lake-atmosphere fluxes of  $\text{CO}_2$ , we leveraged multiple concurrent data sets from a single north temperate lake (Lake Mendota, Wisconsin, USA). This lake has been subject to prior  $\text{CO}_2$  flux investigations (Loken, Crawford, et al., 2019; Reed et al., 2018). Here, we combined flux records based on measurements of  $p\text{CO}_2$  at a moored buoy, measurements distributed across the entire lake surface, EC from a tower located at the end of a narrow peninsula, and FC. The overarching question of this work is: Are lake-atmosphere  $\text{CO}_2$  flux estimates consistent among  $p\text{CO}_2$ , FC, and EC methods? Due to multiple temporal and spatial scales which the independent observations are taken over, we seek to answer the question using (1) analysis of flux distribution over multiple seasons, (2) quantifying cumulative sums of carbon flux, (3) direct comparison of methods, and (4) spectral time series analysis of fluxes.

## 2. Methods

### 2.1. Site Description

Lake Mendota is a well-studied lake located in Southern Wisconsin, USA (43.1°N, 89.4°W) and is part of the North Temperate Lakes Long-Term Ecological Research (NTL-LTER) program. It is dimictic and eutrophic, with a surface area of  $39.9 \text{ km}^2$  and a maximum depth of 25.3 m (mean 12.7 m). The majority of the lake's watershed is composed of agricultural and urban land uses, resulting in elevated nutrient concentrations and high productivity (Carpenter et al., 2007). Thermal stratification typically occurs between May and October and ice cover from late December through March. We defined seasons using water column temperature gradients with spring and fall as periods in which the water column was isothermal, while in summer the lake was thermally stratified.

### 2.2. Flux Estimates

#### 2.2.1. Fixed Point Concentration Gradient Method (F- $p\text{CO}_2$ )

Since 2006, NTL-LTER has managed a monitoring buoy on Lake Mendota that is moored above the lake's deepest point (43.0995°N, 89.4045°W). The buoy is equipped with meteorological and limnological sensors and is deployed seasonally (approximately April through October), capturing the majority of the ice-free season. In 2015, a Turner Designs C-sense  $p\text{CO}_2$  sensor (Turner Designs, San Jose, USA; 0- to 4,000-ppm range, 3% accuracy,  $\pm 120$  ppm) was added to the buoy and installed at 0.5-m depth. For this study, we used wind speed, surface water temperature, and surface  $p\text{CO}_2$  (Magnuson et al., 2019). Wind speed was measured at a height of 2.7 m above the lake surface using an anemometer (R. M. Young Marine Wind Monitor). Water temperature and  $p\text{CO}_2$  were measured at a depth of 0.5 m using a RBR concerto thermistor string and a Turner C-Sense  $\text{CO}_2$  sonde, respectively. Wind speed and water temperature were measured every 30 min, while  $p\text{CO}_2$  was measured every 15 min.  $p\text{CO}_2$  in air was measured from an in situ spectroscopy gas analyzer (Picarro, inc. G2401 Gas Concentration Analyzer) located at a nearby building.

Using data collected at the buoy, we calculated the diffusive efflux of  $\text{CO}_2$  from the lake surface to the atmosphere according to:

$$\text{Flux} = k_{\text{gas}} \times kh \times (p\text{CO}_{2\text{water}} - p\text{CO}_{2\text{air}}) \quad (1)$$

This fixed-point boundary layer method (F- $p\text{CO}_2$ ) is based on the partial pressure gradient between the water ( $p\text{CO}_{2\text{water}}$ ) and the atmosphere ( $p\text{CO}_{2\text{air}}$ ). Multiplying this difference by Henry's law constant

( $kh$ ) converts to molar units and by the gas transfer velocity ( $k_{\text{gas}}$ ) to generate diffusive flux estimates. We estimated  $k_{\text{gas}}$  using concurrent wind speed and water temperature recorded at the buoy following Weyhenmeyer et al. (2012), applying the  $k_{600}$  lake area model and Schmidt model coefficients provided as Model B in Raymond et al. (2013). Henry's law constant ( $kh$ ) was calculated using atmospheric pressure and temperature dependence models provided in Plummer and Busenberg (1982).  $p\text{CO}_2$  flux estimates were computed at 30-min intervals. To temporally match observations between methods, a subset of F- $p\text{CO}_2$  was used from 8 a.m. to 12:00 p.m., the time period that overlapped with the majority (>90%) of the spatially explicit  $p\text{CO}_2$  sampling times (described below).

### 2.2.2. Spatial Concentration Gradient Method (S- $p\text{CO}_2$ )

In addition to the F- $p\text{CO}_2$ -based flux estimation at the buoy, we also compared flux estimates using  $p\text{CO}_2$  measurements from the entire lake surface (S- $p\text{CO}_2$ ). For the entire ice-free period of 2016, Loken, Crawford, et al. (2019) generated  $\text{CO}_2$  efflux estimates at 988 points distributed in a gridded pattern across the lake surface. Efflux estimates were based on measurements of  $p\text{CO}_2$  collected using a boat-mounted water sampling system. Loken, Stanley, et al. (2019) configured a motorboat with water pumps, tubing, a gas equilibrator, a GPS, and water sensors (including a Los Gatos Research Ultraportable Greenhouse Gas Analyzer) to continuously measure (1 Hz) the water surface as the boat traveled across the lake. Bubble free water is extracted from below and in front of any prop created turbulence, with little disturbance to either concentration or flux measurement. S- $p\text{CO}_2$  measurements had an accuracy of  $\pm 0.3$  ppm.

On 26 sampling days spanning the entire ice-free period,  $\sim 10,000$   $p\text{CO}_2$  measurements were collected over an  $\sim 3$ -hr window in the morning. They used the point measurements to interpolate  $p\text{CO}_2$  across the lake surface and, similar to the F- $p\text{CO}_2$  method, calculated efflux using the difference in  $p\text{CO}_2$  between the water and the air. To match the spatial  $p\text{CO}_2$  data set, Loken, Crawford, et al. (2019) used a spatially explicit  $k$  model (Vachon et al., 2013), which takes into account wind speed and direction and allows  $k$  to vary across the lake surface. Daily  $p\text{CO}_2$  at each of the 988 points were estimated by temporal interpolation, which they combined with daily spatially explicit  $k$  estimates to calculate daily efflux. Two subsets of S- $p\text{CO}_2$  data were used to quantify spatial variability, 10 stratified random points from the entire lake and S- $p\text{CO}_2$  measurement locations from within the EC footprint.

Both F- $p\text{CO}_2$  and S- $p\text{CO}_2$  methods depend on wind speed for accurate  $k$  estimates. Wind data for this work have an accuracy of  $0.3 \text{ m s}^{-1}$ .  $k$  accuracy varies in time and space but is approximated to be  $0.6 \text{ cm hr}^{-1}$ . With both methods using the same wind speed for their  $k$  estimates, there is a small degree of dependence between the methods.

### 2.2.3. Flux Chamber Diffusion Method (FC)

We conducted four FC campaigns between 6 July 2017 and 24 April 2018.  $\text{CO}_2$  sensors (Sensair K30,  $\pm 30$  ppm) were installed inside floating plastic chambers with a foam collar of diameter 0.3 m and a height of 0.12 m. Flux rates were calculated using the chamber dimensions (surface area and volume) and continuous  $p\text{CO}_2$  measurements within the enclosed headspace. Each 24-hr sampling campaign consisted of seven sampling trips spaced every 4 hr with the goal of measuring flux rates over a complete diel cycle. For each measurement, we placed two chambers on the lake surface in the middle of the lake (same location as the buoy) and let them drift for 5 min. We repeated the FC procedure three times per chamber and calculated the average of the six flux measurements.  $\text{CO}_2$  flux was calculated as follows:

$$\text{Flux} = \frac{\Delta p\text{CO}_2}{\Delta t} \times \frac{V}{SA} \quad (2)$$

where  $V$  is the chamber volume ( $0.03114 \text{ m}^3$ ),  $SA$  is the chamber bottom area ( $0.071 \text{ m}^2$ ), and  $t$  is time (s). Prior to the first campaign, we calibrated all sensors using  $\text{N}_2$  gas and the "zero calibration" method per Bastviken et al. (2015). For all subsequent campaigns we re-confirmed the zero  $\text{CO}_2$  readings using  $\text{N}_2$  gas.

### 2.2.4. EC Method

EC flux observations (Ameriflux site: US-PnP, doi: 10.17190/AMF/1433376) were collected from a tower at the end of an  $\sim 50$ -m-wide peninsula on the shore of Lake Mendota (Figure 1) starting on 20 June 2016. These flux observations were made with a sonic anemometer (CSAT3, Campbell Scientific, Logan UT, USA) and open-path infrared gas analyzer for  $\text{CO}_2$  and water vapor gas concentration (LI-7500A, Li-Cor, Lincoln,



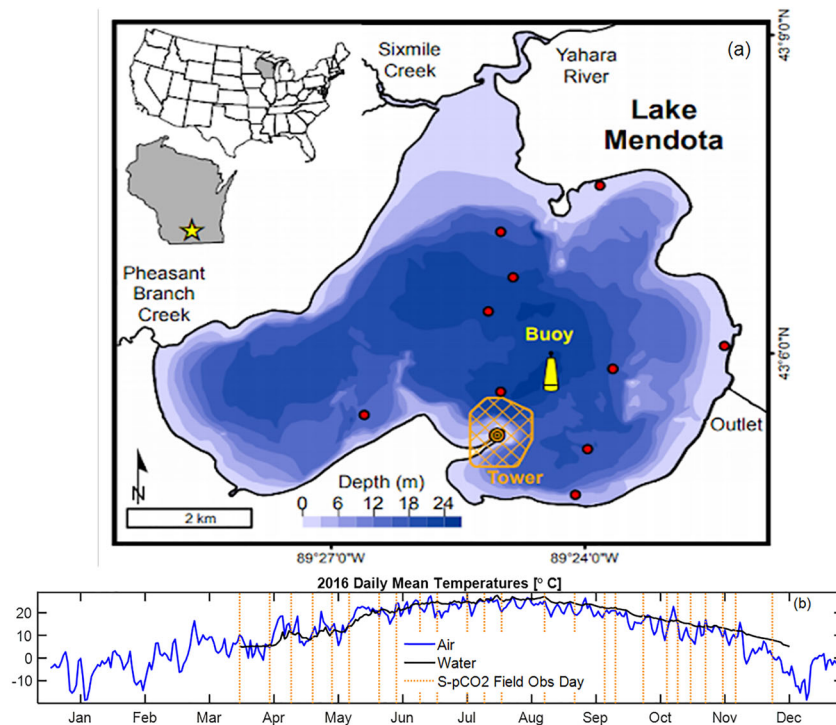


**Figure 1.** (a) Lake Mendota. Buoy (yellow) is deployed in the deepest part of the lake and is the location for the  $F\text{-}p\text{CO}_2$  and FC flux estimates. The red circles are a stratified selection of data points from the S- $p\text{CO}_2$  method used in Figure 5. Grid section (orange with a center circle) of EC tower location and 1- $\text{km}^2$  footprint. (b) 2016 average daily air (blue) and surface water (black) temperatures. Spatial gradient concentration measurements were taken on the 2016 days of year indicated by the (25 orange) vertical lines. Dashed line (gray) at 20°C used to symbolize phenology. Summer stratification is generally when surface waters were above 20°C, while spring and fall mixing occurred below this water temperature.

NE, USA,  $\pm 5$  ppm) at a height of 12.4 m above the lake on a 0.95-m boom, along with measurements of air temperature and humidity (Vaisala, Inc. HMP45C). Measurements of incoming solar radiation and atmospheric pressure were collected from a nearby meteorological tower located on the roof of the Atmospheric, Oceanic, and Space Sciences building at the University of Wisconsin.

Eddy fluxes were calculated based on the covariance of vertical wind velocity and scalar concentrations following the approach of Mauder and Foken (2015), with quality control flags for stationarity, integral turbulence, and propagate estimates of random error. Typical corrections were applied, including planar fit rotation, and Webb-Pearson-Leuning density corrections, except for  $u^*$  filtering. A change point detection method is not possible, given the dependence of flux on  $u^*$  and instead we use a fix value for cutoff ( $0.1 \text{ m s}^{-1}$ ). Gap filling was performed using the Marginal Distribution Smapping (MDS) method with REddyProc (Reichstein et al., 2005), with uncertainty estimated using both random uncertainty methods for turbulent flux sampling (Salesky et al., 2012) and gap filling (Moffat et al., 2007). Using an eddy flux surface flux footprint model (Kljun et al., 2015), we identified and removed non-lake data at 30-min timescales, primarily when winds were from the forested portion of the peninsula. After footprint screening and quality control, 26% of data were retained. Lacking a concentration gradient profile, below-sensor storage fluxes were not measured and are assumed to average to zero at the daily scale (Xu et al., 2019), which is common at most sites.

### 2.3. Comparison of Methods

Flux estimates varied in temporal and spatial coverage (Table 1). EC-based fluxes were collected continuously since 2016. Buoy-based  $F\text{-}p\text{CO}_2$  estimates are also continuous since this time, with the exception of winter months. We only have S- $p\text{CO}_2$  rates for the ice-free period of 2016, which were collected approximately weekly and daily rates that were modeled by interpolating  $p\text{CO}_2$  through time

**Table 1**  
*Temporal Duration, Water/Gas Sampling Frequency, and Spatial Extent and Resolution for the Four Methods Used to Estimate CO<sub>2</sub> Fluxes in Lake Mendota Between 2016 and 2018, Along With Data Availability Information*

Method	Measurement period	Sampling frequency	Spatial extent	Spatial resolution	Citation
Fixed point concentration gradient (F- <i>p</i> CO <sub>2</sub> )	Open water seasons (approx. April–October) 2016–2018	15 min	Single point	10 cm <sup>3</sup>	Magnuson et al. (2019)
Spatial concentration gradient (S- <i>p</i> CO <sub>2</sub> )	March–December 2016	14 days	Whole lake	200 m <sup>2</sup>	Loken, Stanley, et al. (2019)
Flux chamber diffusion (FC)	Four measurement campaigns, July 2017 to April 2018	5-min sampling, every 4 hr for 24 hr	Single point	0.28 m <sup>2</sup>	A. R. Desai (2019)
Eddy covariance (EC)	June 2016 to August 2018	30 min	1 km <sup>2</sup>	1 km <sup>2</sup>	A. Desai (2018)

(see Loken, Crawford, et al., 2019 for details). Thus, these three data sources (S-*p*CO<sub>2</sub>, F-*p*CO<sub>2</sub>, and EC) overlapped from June to December 2016. We collected FC flux rates seasonally starting in summer 2017 (28–29 July 2017, 28–29 October 2017, and 23–24 April 2018). In addition to temporal overlap, we must also consider spatial coverage as sampling sites varied among methods. Both the FC- and F-*p*CO<sub>2</sub>-based rates were determined at the center of the lake. The EC rates reflect the area surrounding the tower along the lake's southern shoreline, and S-*p*CO<sub>2</sub> covered the entire lake surface (Figure 1).

Because of varying temporal resolution among data sets, we converted all data sets to daily averages, representing the coarsest temporal scale. Using the S-*p*CO<sub>2</sub> flux estimates, we generated two additional spatial data sets. First, we randomly selected 10 stratified points from the entire lake to visualize spatial variability across the lake (S-*p*CO<sub>2</sub> Stratified Points). Second, we subset the S-*p*CO<sub>2</sub> data set by only including flux estimates from within the EC footprint (S-*p*CO<sub>2</sub> Tower Footprint) for a comparison between these two methods that was not confounded by differences in sampling areas. Cumulative fluxes from 2016 were calculated from F-*p*CO<sub>2</sub>, S-*p*CO<sub>2</sub>, and EC observations. For the entire study period, the S-*p*CO<sub>2</sub> data had 17% of data functionally usable (26 sampling days over the growing season), F-*p*CO<sub>2</sub> had 86% data retained, and as previously mentioned, 26% of EC data were retained.

In addition to comparing similarity in seasonal pattern and magnitude, we also wanted to determine if the different methods exhibited similar temporal variance. To do so, we calculated a fast Fourier power spectrum for EC, S-*p*CO<sub>2</sub>, and F-*p*CO<sub>2</sub> gap-filled daily net ecosystem exchange. Buoy winter fluxes were assumed to be zero for the purpose of this analysis. Data analysis was done in Matlab R2019a and IDL 8.6.0.

### 3. Results

#### 3.1. Patterns Among Methods

Footprint modeling revealed that the EC footprint originated primarily from open water, with very little apparent input from the terrestrial peninsula (Figure 2a), with the distance of maximum contribution of fluxes on average being 40 m, while the distance containing 80% of flux contribution was 410 m. Friction velocity (*u*<sup>\*</sup>) values were high due to winds crossing the peninsula, showing increased turbulence due to the tree canopy (Figure 2b). While winds originated from all directions, wind speeds were lower over the peninsula as well (Figure 2c). These factors combined to limit the footprint along the narrow range of wind directions over the peninsula.

In all years, F-*p*CO<sub>2</sub> flux estimates followed a similar pattern of near zero or slightly negative fluxes denoting CO<sub>2</sub> movement from the atmosphere to the lake during spring and summer months before becoming strongly positive (net CO<sub>2</sub> efflux from the lake to the atmosphere) in the fall (Figures 3 and 4). Daily-averaged fluxes varied from  $-1.2$  to  $4.1 \mu\text{m m}^{-2} \text{s}^{-1}$  across all dates with a SD of 0.62. This same pattern was also demonstrated by the S-*p*CO<sub>2</sub> method (Figures 3 and 4), and flux estimates were similar in magnitude and direction as the F-*p*CO<sub>2</sub> results in 2016 ( $-0.39$  to  $1.6 \mu\text{m m}^{-2} \text{s}^{-1}$ , SD of 0.36). The limited set of FC deployments also followed the same general pattern of CO<sub>2</sub> influx to the lake in spring, a weaker influx during summer, and efflux in the fall (Figures 3b–3d). However, the range of FC flux values was wider than for the two *p*CO<sub>2</sub>-based methods ( $-22.5$  to  $18.1 \mu\text{m m}^{-2} \text{s}^{-1}$ , CV of 2.51).

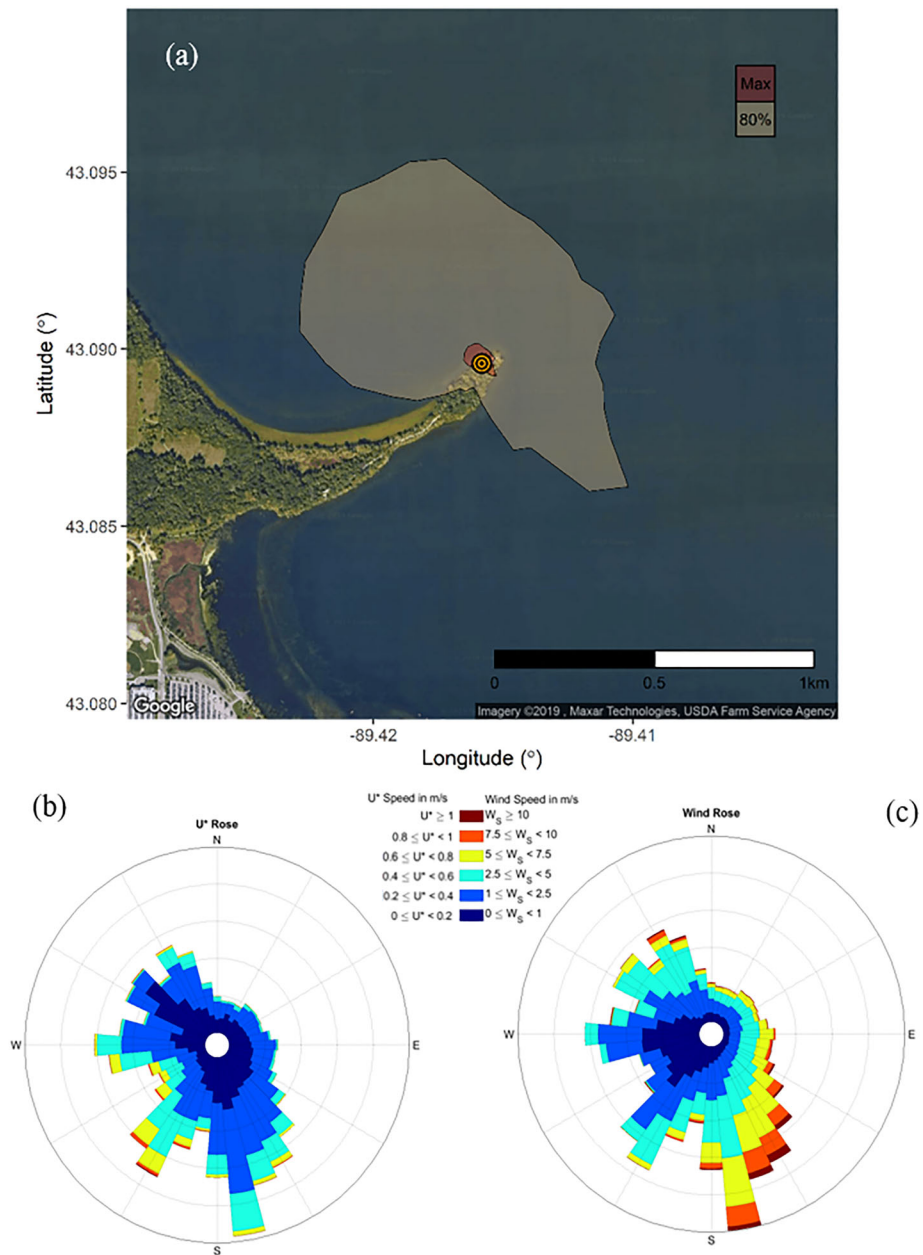


**Figure 2.** Map of picnic point EC tower and contributing footprint showing the distance of maximum flux and distance of 80% of the footprint (a). Average friction velocity ( $u^*$ , b) and wind speed (c) measured from the eddy covariance tower, shown in  $10^\circ$  bins.

Fluxes derived from the EC method were characterized by higher variation, often shifting from negative to positive fluxes within a period of 1–3 days. Daily-averaged fluxes varied from  $-22.5$  to  $18 \mu\text{m m}^{-2} \text{s}^{-1}$ , and the coefficient of variation was 3.13. There were no clear seasonal patterns in terms of magnitude, direction, or variance although large  $\text{CO}_2$  uptakes were recorded prior to ice-on in both 2016 and 2017, and negative and smaller positive fluxes were more common during ice-covered winter days.

### 3.2. Comparisons Among Methods

Differences among methods were clearly illustrated when flux data were expressed as cumulative flux (Figure 5). All methods indicated that the lake was a slight  $\text{CO}_2$  sink over the summer; however, estimates diverged substantially during fall. Both the S- $p\text{CO}_2$  and F- $p\text{CO}_2$  methods consistently indicated  $\text{CO}_2$  flux into

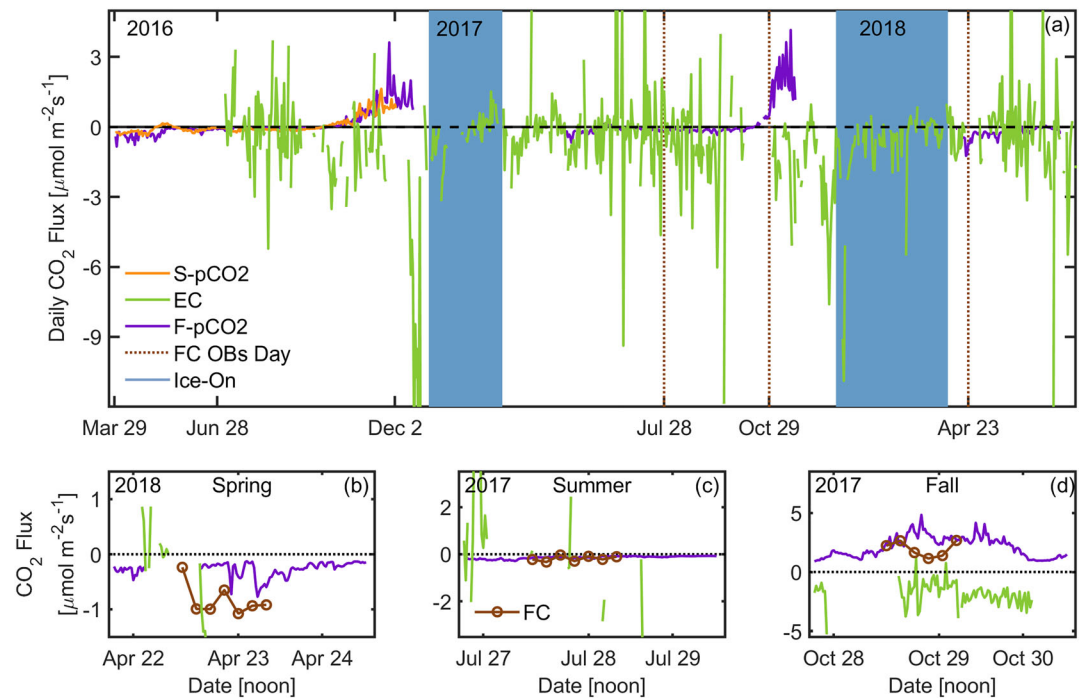


**Figure 3.** (a) Multi-year time series of mean daily CO<sub>2</sub> flux. F-pCO<sub>2</sub>, fixed gradient concentration method, recorded from a stationary buoy (purple), S-pCO<sub>2</sub>, spatial gradient concentration method, recorded by a moving boat (orange), and eddy covariance (green). Dates of flux chamber measurements shown as brown dotted vertical line. (b–d) Hourly 3-day subsets from spring, summer, and fall, centered on when FC data were collected. F-pCO<sub>2</sub> (purple) and EC (green) being 30-min data and FC (brown) are every 4 hr for a diel cycle.

the lake all summer and substantial CO<sub>2</sub> flux out of the lake during fall. At the end of the year, the cumulative flux based on F-pCO<sub>2</sub> was 15% higher (43.4 vs. 37.7 gC m<sup>-2</sup>) than flux based on S-pCO<sub>2</sub>, but both followed similar temporal trends. In contrast, the EC method suggested that the lake fluctuated between CO<sub>2</sub> source and sink behavior with a high degree of variability on the weekly timescale. At the end of summer (day ~268), the EC-based cumulative flux was comparable to the boundary layer-based rates. However, during fall, once mixing begins, the EC cumulative flux became progressively more negative, suggesting that the lake became a more substantial CO<sub>2</sub> sink.

CO<sub>2</sub> fluxes based on FC (flux chamber) agreed in magnitude and direction with the F-pCO<sub>2</sub> during spring, summer, and fall (Figures 3b–3d). Comparing FC with EC, the two methods disagreed in flux magnitude during summer and direction during fall.

The discrepancy between methods could be caused by the temporal or spatial resolution of observations. The daytime EC data more closely aligned with the F-pCO<sub>2</sub> and S-pCO<sub>2</sub> result during the summer. These methods agreed that the daytime flux of CO<sub>2</sub> during the summer was consistently into the lake. During the fall, the daytime EC fluxes remained negative, suggesting a consistent flux of CO<sub>2</sub> into the lake. Spatially, the S-pCO<sub>2</sub> results within the EC footprint were consistent with the majority of the S-pCO<sub>2</sub> data. This suggests the lake was relatively homogeneous in regard to flux rates, with subset S-pCO<sub>2</sub> locations showing ~20% variability in accumulated fluxes at the end of the year. Temporal subsets of EC data show differences during the summer with the full day EC data but ultimately small differences in accumulated fluxes at the end of the year. Average EC error was 38.9%, with larger accumulated errors during the fall.

Directly comparing estimates using linear regression models further demonstrates the dissimilarity among methods. The two concentration gradient methods, F-pCO<sub>2</sub> and S-pCO<sub>2</sub>, agreed in magnitude and direction ( $R^2 = 0.58$ ,  $p$  value < 0.001; Figure 6a). When flux estimates were categorized by season, data from the summer were tightly clustered, while data from the fall were more scattered. Comparing EC to S-pCO<sub>2</sub> (Figure 6b), there was poor agreement ( $R^2 = 0.07$ ;  $p = 0.03$ ), and the regression model had a negative slope. Thus, daily flux rates using EC disagreed in direction with the concentration-based methods.



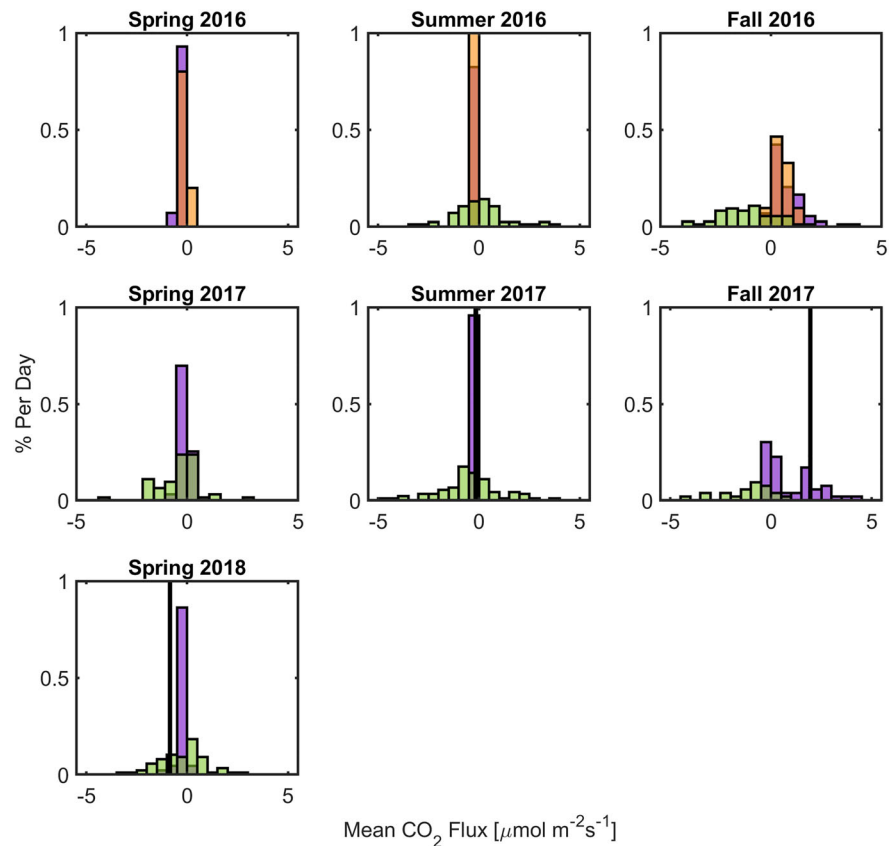


**Figure 4.** Histograms of seasonal daily CO<sub>2</sub> gas fluxes. Spatial S-*p*CO<sub>2</sub> fluxes (orange), fixed F-*p*CO<sub>2</sub> fluxes (purple), and EC fluxes (green) for spring 2016 to spring 2018 and three seasons of FC mean fluxes in 2016 (brown).

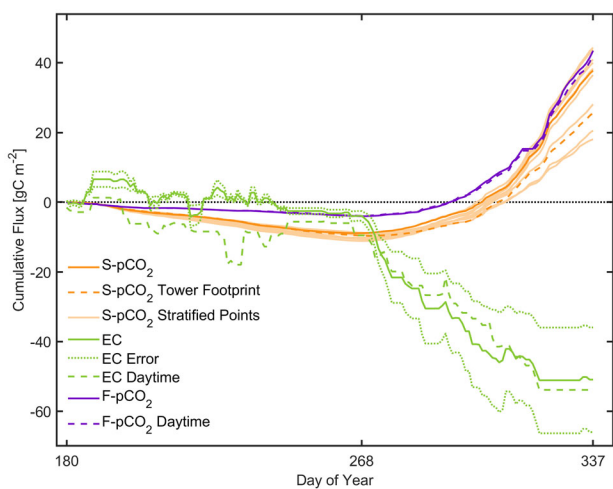


**Figure 5.** Cumulative summation of lake-atmosphere CO<sub>2</sub> fluxes. Flux estimates using the S-*p*CO<sub>2</sub> method (bold orange), from 10 random points across the lake (orange), and within the tower footprint (orange dashed line), EC (green), and EC only during day (8 a.m. to 12 p.m., green dashed line) and the F-*p*CO<sub>2</sub> method (purple), and fixed boundary layer method during the day (8 a.m. to 12 p.m., purple dashed line).

Fourier power spectral decomposition (Figure 7) of daily flux from EC, F-*p*CO<sub>2</sub>, and S-*p*CO<sub>2</sub> data all had similar patterns over the quantifiable frequencies, with highest spectral power seen in EC time series, S-*p*CO<sub>2</sub>, and finally F-*p*CO<sub>2</sub>. Seasonal and synoptic (3–10 days) variability dominate all three, though the EC tower also shows a sub-monthly (~20 day) mode of variability not seen in the other two.

#### 4. Discussion

Few studies have used multiple measurements of multi-year lake-atmosphere fluxes to address systemic biases in methods. Using concurrent multi-year records from a single lake, we showed divergent behavior among flux estimates, particularly during the fall turnover period. EC-based calculations had large and opposing sign CO<sub>2</sub> flux estimates compared to FC and concentration gradient-based methods (F-*p*CO<sub>2</sub> and S-*p*CO<sub>2</sub>). FC-based methods agreed in direction and magnitude as *p*CO<sub>2</sub>-based methods; however, we lack sufficient FC coverage to interrogate the validity of this agreement. Together, these results suggest that at least for this lake and these estimates, EC and concentration gradient methods for estimating CO<sub>2</sub> flux differ dramatically.

The spatial and buoy-based concentration gradient estimates closely agreed. Both estimates followed similar seasonal patterns, indicating

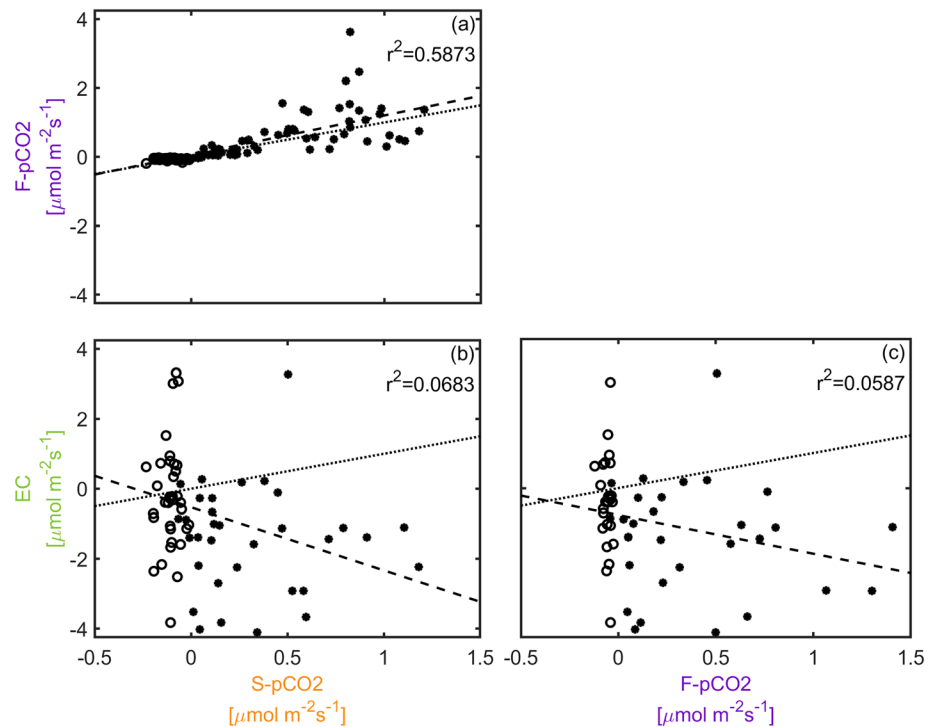


**Figure 6.** Daily mean S-pCO fluxes versus F-pCO<sub>2</sub> (a) and EC (b) and F-pCO<sub>2</sub> versus EC (c). Summer data are plotted as open circles, fall data as \*. Linear regression line (dashed) and one-to-one line (dotted). Statistics (*p* and *R*<sup>2</sup>) for linear regression included.

that the lake was taking in CO<sub>2</sub> from the atmosphere during the summer and emitted a substantial amount during the fall. The buoy-based data showed this seasonal phenology in three consecutive years (Reed et al., 2018), aligning with other studies of productive lakes (Maberly, 1996) and the perception that productive lakes behave as CO<sub>2</sub> sinks during the summer (Balmer & Downing, 2011). The agreement between the spatial and buoy-based concentration data suggests low spatial heterogeneity in CO<sub>2</sub> fluxes

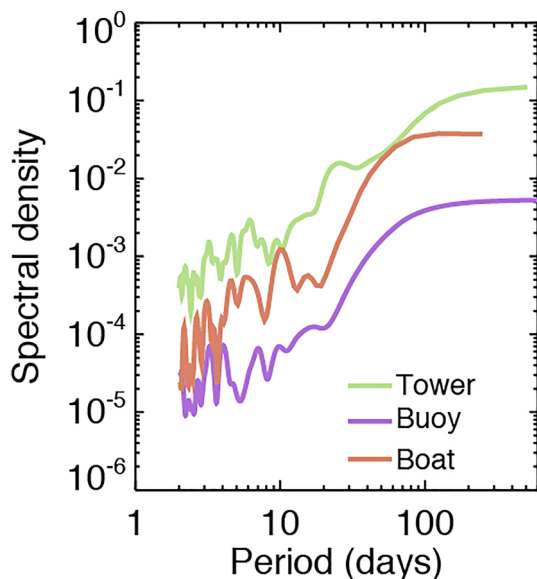


**Figure 7.** Fourier power spectral decomposition of daily EC (green), F-pCO<sub>2</sub> (purple), and S-pCO<sub>2</sub> (orange) CO<sub>2</sub> flux.

across the surface of Lake Mendota. On average most of the lake surface was within a 0.2 μmol m<sup>-2</sup> s<sup>-1</sup> range in CO<sub>2</sub> flux (Loken, Crawford, et al., 2019). Low spatial heterogeneity in CO<sub>2</sub> concentration may reflect the lake's high buffering capacity, which would dampen variation in CO<sub>2</sub> caused by spatial heterogeneity in metabolic processes (Loken, Crawford, et al., 2019). Spatial variability in CO<sub>2</sub> flux is small compared to the seasonal variability from all our CO<sub>2</sub> flux methods (Figures 3 and 5). However, spatial heterogeneity increased during fall turnover, making the buoy location less representative of the whole lake during this period (Loken, Crawford, et al., 2019). During periods of chaotic water mixing, the representativeness of a single location decreases (Erkkila et al., 2018). Thus, we suspect that the discrepancies among methodologies during the summer season are not due to spatial heterogeneity in gas exchange across the lake surface.

With a limited number of FC observations, FC data approximately matched F-pCO<sub>2</sub> and S-pCO<sub>2</sub> during the spring and summer. Comparing FC and F-pCO<sub>2</sub> methods, López Bellido et al. (2009) and Vachon et al. (2010) found that FCs were systematically higher than F-pCO<sub>2</sub>, due to site- and time-specific gas transfer velocities and chamber effects on water turbulence. They used daily concentration measurements and hence were not able to access daily patterns. Podgrajsek et al. (2014)

found that FC and EC fluxes generally agreed, except when  $p\text{CO}_2$  varied within the EC footprint. This is expanded on to show higher EC-derived  $\text{CO}_2$  fluxes at night relative to F- $p\text{CO}_2$  and also that F- $p\text{CO}_2$  methods need to account for convection within the water column (Podgrajsek et al., 2016). Both of these studies show that the high degree of spatial and temporal variability of water-atmosphere fluxes and differences between methods, in their case, could be explained by difference in measurement footprint areas. Erkkila et al. (2018) found that F- $p\text{CO}_2$ -based estimates were lower than EC, while those based on FC were higher than EC estimates. Together, there does not appear to be an emerging trend among results, other than EC fluxes can be typically higher at night, hinting at possibility of convective gas transfer or some sort of decoupling of lake surface to EC measurement height.

$k$  may be responsible for the discrepancy among flux estimates. The  $k$  model underlying our concentration gradient-based methods may have not adequately portrayed turbulence at the lake surface. Convective mixing within the water column introduces error into F- $p\text{CO}_2$  methods (Podgrajsek et al., 2016). Our models base  $k$  on wind speed, but the effects of individual wind events on lakes are highly variable. For example, 2 days with similar wind speed and direction likely does not have the identical patterns of surface turbulence and our models lack resolution at fine spatial scales (Loken, Crawford, et al., 2019). While only using short periods (1–3 days), Eugster et al. (2003) used EC and chambers from Alaska and Switzerland to show the importance of convective mixing due to lake-atmosphere fluxes, with significant differences between methods during periods of stratification and with deep, penetrative convection. Ultimately, concentration gradient-based estimates rely on measurements of wind and/or water density collected at a single location to represent  $k$  over the whole lake, adding uncertainty to gas efflux estimates. Here, both concentration gradient fluxes depend on the same wind speed measurement, removing true independence between the two.

Variations in lake mixing depth and potential periods of stratification could explain differences. Here, with a relatively large and windy lake, this seems unlikely. During periods of higher stratification, methods typically agree. Only during the fall, when there is full-lake mixing do we see the large differences between the EC and gradient methods. So while this could be one source of error, it would appear to be limited in absolute size.

Another possible source of uncertainty is rapid buffering in the upper layer of the water column. Any potential buffering would be unlikely to persist over time, and that bias should be predictable based on mixed (e.g., wind speed) or alkalinity lake conditions. The S- $p\text{CO}_2$  data are sampled close to the surface, where buffering would be limited, and with the good agreement between S- $p\text{CO}_2$  and F- $p\text{CO}_2$  methods, the possibility is unlikely.

Buoyancy-driven turbulence is more important than wind-driven turbulence in smaller lakes (Read et al., 2012) and at night (Podgrajsek et al., 2014). While both wind-driven and convective turbulence play roles in gas exchange in Lake Mendota, wind shear is likely a bigger factor in this present study due to the size of the lake. With a large fetch and relatively steady winds, we do not expect convection to be a major driver of gas exchange in Lake Mendota. Comparing  $k$  among lakes, smaller lakes have a bigger contribution from convective mixing, while for larger lakes Read et al. (2012) argue that wind is more important. However, the influence of convective mixing may be more important near shore, at night, and during fall turnover. All three factors may provide some clues why the EC estimate diverges so dramatically from the other methods. The EC tower is located near two relatively shallow bays, where thermal convection may cause an increase in  $k$  and flux at night. Further, these bays may have irregular currents and breaking waves, which may elicit further enhancement of flux rates within the tower footprint. How these periods align with  $\text{CO}_2$  saturation would determine the actual flux rates in the footprint. Modeling water currents and convective mixing within the tower footprint is challenging and would require a high-resolution whole lake three-dimensional model. We currently lack data at fine-scale resolution in lakes to fully model  $k$  in lakes, which remains an open challenge. While the EC data seem like a promising tool to capture this fine-scale variation in gas exchange, additional methodology developments are needed.

With an increase in the availability of oxygen data and the derived oxygen flux estimates, potential errors in carbon flux measurements can be highlighted by dissolved oxygen (DO). Reed et al. (2018) showed DO fluxes to be more variable than EC  $\text{CO}_2$  fluxes but largely agreeing over the summer and fall seasons. Using EC measured  $\text{CO}_2$  fluxes and DO data, Morin et al. (2018) found microbial activity and DO to be more connected to  $\text{CO}_2$  outgassing, relative to net  $\text{CO}_2$  exchange. Timescales for these works are often large, and more

research on connecting DO and EC fluxes in smaller timescales could show additional light on net CO<sub>2</sub> exchange.

Another possible explanation is potential biases in EC measurements during periods of low turbulence, complex turbulence, or advection in the atmosphere. Morin et al. (2018) noted in a model study the role of tower height and lake-land circulations in driving eddy transport that would bias traditional flux calculation based on half-hourly Reynold's decomposition. As the surface cools, enhanced low-level atmospheric stability may suppress turbulence, leading to larger than typical storage or advective contribution to surface fluxes (Lee et al., 2004). As noted by Xu et al. (2019), below-sensor storage flux calculation can be critical to correcting tower-measured flux to represent surface flux, especially periods around sunrise and sunset. However, while we lack storage flux observations at this site or models of local circulation and turbulence on the peninsula, there is no evidence in the data of a preferential circulation during fall or other periods of stable conditions. Further work on data quality filtering of EC is necessary to build confidence in its use over lakes.

EC may have other benefits, even when subject to potential systematic bias. Here, when examining the spectral density of the multiple observations, the EC observations show a 20- to 30-day frequency not observed by the other methods, including the similarly high-frequency buoy measurements. Eugster et al. (2003) also conclude that EC methods should be used in order to collect process-scale data from the full season. Similarly, Podgrajsek et al. (2016) suggest that the high temporal resolution of EC is crucial to resolve diel changes in flux, combined with measurements within the water column with high (30 min) frequency. Reed et al. (2018) used a different EC observation data set on Lake Mendota, not used here due to a large amount of gaps from that tower's location during the study period, which showed high degrees of coherence between CO<sub>2</sub> flux and air temperature at a similar sub-monthly (20–30 days) timescale. An emerging trend in aquatic flux literature explores this monthly timescale of variation where Liu et al. (2011) and Liu et al. (2016) connect synoptic weather patterns to mixing, and Shao et al. (2015) and Ouyang et al. (2017) show monthly correlation between CO<sub>2</sub> flux and chlorophyll and algal blooms.

There are ways to capture this 20- to 30-day timescale without high temporal coverage. Previously, Natchimuthu et al. (2016) used a multi-year FC data set and then sub-sampling the observations following the methods of Wik et al. (2016). They concluded that only  $\geq 8$  measurement days, distributed over multiple seasons, and high enough spatial coverage ( $\geq 8$  locations during summer,  $\geq 5$  during spring and fall) are key for representative ( $\pm 20\%$ ) flux estimates at the annual timescale. However, they note that the flux estimates would be biased if observations excluded episodic events such as lake circulation patterns, diel or seasonal variation, or high flux areas from a lake. There is a mismatch between what the EC literature is concluding about needing high temporal resolution observations and the FC literature about only needing  $\geq 8$  days for CO<sub>2</sub> flux estimates (Natchimuthu et al., 2016). We argue that while it may be possible to estimate annual fluxes from a small number of sample days, functionally, we think it would be difficult to observe only 8 days of FC fluxes and have a high degree of confidence that we have captured the temporal processes needed. Ultimately, we do judge the flux signal found at the 20- to 30-day frequency as important and the best way to capture appears to be EC methods.

## 5. Conclusions

While major advances have been made, quantifying lake-atmosphere fluxes from individual lakes over multiple spatial and temporal scales remains a challenge. Lakes are an important factor in carbon cycling at both global and local scales. Accurately accounting for temporally and spatially heterogeneity in the flux of carbon across lake surfaces is vital for incorporation and constraining process-based predictions within lake models.

Overall, there is a need for increased spatiotemporal resolution in studies of CO<sub>2</sub> exchange between lakes and the atmosphere. Multi-year temporal data collection is essential to capture, diel, monthly, and seasonal patterns. Spatially, there is still an open question as to which method is capturing flux magnitude correctly, as each method integrates different processes into the observation. This is done most explicitly when choosing between multiple  $k$  models but is also implicated when screening EC data. There is no emerging trend in magnitude or direction between methods, and additional work is needed to bridge spatiotemporal scales.



## Conflict of Interests

The authors declare no competing financial interests.

## Data Availability Statement

Data for eddy covariance (US-PnP) can be found at Ameriflux (<https://doi.org/10.17190/AMF/1433376>). CO<sub>2</sub> concentrations used in the spatial (data set 337, <https://doi.org/10.6073/pasta/fe9c5437f67254f521bf5-f7e0308bf93>) and temporal concentration gradient (data set ID 129, <https://doi.org/10.6073/pasta/9bced2f6f-f81aa30f0f573766c0a410b>) can be found at the NTL-LTER database (<https://lter.limnology.wisc.edu/data>) and are indexed in the Environmental Data Initiative. Floating chamber data have been deposited into the Environmental Data Initiative database (<https://doi.org/10.6073/pasta/f6a915989753aba6f18b6b095e7a52d0>).

## Acknowledgments

This study was supported by the National Science Foundation (NSF) Atmospheric and Geospace Sciences Postdoctoral Fellowship Program (GEO-1430396) and the NSF Long-Term Ecological Research (LTER) program award to North Temperate Lakes (NTL) (DEB-1440297). We would like to thank Jonathan Thom for field work help, Yost R. for keeping momentum going on the project, and John Maginnis for his perseverance and assistance on the FC 2017-18 campaigns. We thank Mark Johnson and one anonymous reviewer for their thoughtful peer review comments.

## References

- Balmer, M. B., & Downing, J. A. (2011). Carbon dioxide concentrations in eutrophic lakes: Undersaturation implies atmospheric uptake. *Inland Waters*, 1(2), 125–132. <https://doi.org/10.5268/IW-1.2.366>
- Bastviken, D., Sundgren, I., Natchimuthu, S., Reyier, H., & Gålfalk, M. (2015). Cost-efficient approaches to measure carbon dioxide (CO<sub>2</sub>) fluxes and concentrations in terrestrial and aquatic environments using mini loggers. *Biogeosciences*, 12(12), 3849–3859. <https://doi.org/10.5194/bg-12-3849-2015>
- Biddanda, B. (2017). Global significance of the changing freshwater carbon cycle. *Eos*. <https://doi.org/10.1029/2017EO069751>
- Carpenter, S. R., Benson, B. J., Biggs, R., Chipman, J. W., Foley, J. A., Golding, S. A., et al. (2007). Understanding regional change: A comparison of two lake districts. *Bioscience*, 57(4), 323–335. <https://doi.org/10.1641/B570407>
- Chmiel, H. E., Hofmann, H., Sobek, S., Efreanova, T., & Pasche, N. (2019). Where does the river end? Drivers of spatiotemporal variability in CO<sub>2</sub> concentration and flux in the inflow area of a large boreal lake. *Limnology and Oceanography*, 65(6), 1161–1174.
- Cole, J. J., & Caraco, N. F. (1998). Atmospheric exchange of carbon dioxide in a low-wind oligotrophic lake measured by the addition of SF<sub>6</sub>. *Limnology and Oceanography*, 43(4), 647–656. <https://doi.org/10.4319/lo.1998.43.4.0647>
- Cole, J. J., Prairie, Y. T., Caraco, N. F., McDowell, W. H., Tranvik, L. J., Striegl, R. G., et al. (2007). Plumbing the global carbon cycle: Integrating inland waters into the terrestrial carbon budget. *Ecosystems*, 10(1), 172–185. <https://doi.org/10.1007/s10021-006-9013-8>
- Cory, R. M., Ward, C. P., Crump, B. C., & Kling, G. W. (2014). Carbon cycle. Sunlight controls water column processing of carbon in arctic fresh waters. *Science*, 345(6199), 925–928. <https://doi.org/10.1126/science.1253119>
- Crawford, J. T., Loken, L. C., Casson, N. J., Smith, C., Stone, A. G., & Winslow, L. A. (2015). High-speed limnology: Using advanced sensors to investigate spatial variability in biogeochemistry and hydrology. *Environmental Science & Technology*, 49(1), 442–450. <https://doi.org/10.1021/es504773x>
- Crusius, J., & Wanninkhof, R. (2003). Gas transfer velocities measured at low wind speed over a lake. *Limnology and Oceanography*, 48(3), 1010–1017. <https://doi.org/10.4319/lo.2003.48.3.1010>
- Denfeld, B. A., Ricão Canelhas, M., Weyhenmeyer, G. A., Bertilsson, S., Eiler, A., & Bastviken, D. (2016). Constraints on methane oxidation in ice-covered boreal lakes. *Journal of Geophysical Research: Biogeosciences*, 121, 1924–1933. <https://doi.org/10.1002/2016JG003382>
- Desai, A. (2018). AmeriFlux US-Pnp Lake Mendota, picnic point site, edited; AmeriFlux; University of Wisconsin Madison.
- Desai, A. R. (2019). GLEON DC-FLUX lake Mendota floating chamber carbon dioxide flux, 2017–2018, *Environmental Data Initiative*.
- Duarte, C. M., Prairie, Y. T., Montes, C., Cole, J. J., Striegl, R., Melack, J., & Downing, J. A. (2008). CO<sub>2</sub> emissions from saline lakes: A global estimate of a surprisingly large flux. *Journal of Geophysical Research*, 113, G04041. <https://doi.org/10.1029/2007JG000637>
- Duc, N. T., Silverstein, S., Lundmark, L., Reyier, H., Crill, P., & Bastviken, D. (2012). Automated flux chamber for investigating gas flux at water–air interfaces. *Environmental Science & Technology*, 47(2), 968–975. <https://doi.org/10.1021/es303848x>
- Dugan, H. A., Woolway, R. I., Santoso, A. B., Corman, J. R., Jaimes, A., Nodine, E. R., et al. (2016). Consequences of gas flux model choice on the interpretation of metabolic balance across 15 lakes. *Inland Waters*, 6(4), 581–592. <https://doi.org/10.1080/IW-6.4.836>
- Erkkila, K.-M., Ojala, A., Bastviken, D., Biermann, T., Heiskanen, J. J., Lindroth, A., et al. (2018). Methane and carbon dioxide fluxes over a lake: Comparison between eddy covariance, floating chambers and boundary layer method. *Biogeosciences*, 15(2), 429–445. <https://doi.org/10.5194/bg-15-429-2018>
- Eugster, W., Kling, G., Jonas, T., McFadden, J. P., Wüest, A., MacIntyre, S., & Chapin, F. S. III (2003). CO<sub>2</sub> exchange between air and water in an Arctic Alaskan and midlatitude Swiss lake: Importance of convective mixing. *Journal of Geophysical Research*, 108(D12), 4362. <https://doi.org/10.1029/2002JD002653>
- Jonsson, A., Åberg, J., Lindroth, A., & Jansson, M. (2008). Gas transfer rate and CO<sub>2</sub> flux between an unproductive lake and the atmosphere in northern Sweden. *Journal of Geophysical Research*, 113, G04006. <https://doi.org/10.1029/2008JG000688>
- Kitaigorodskii, S., & Donelan, M. A. (1984). Wind-wave effects on gas transfer. In *Gas transfer at water surfaces*, edited (pp. 147–170). New York: Springer.
- Kljun, N., Calanca, P., Rotach, M. W., & Schmid, H. P. (2015). A simple two-dimensional parameterisation for Flux Footprint Prediction (FFP). *Geoscientific Model Development*, 8(11), 3695–3713. <https://doi.org/10.5194/gmd-8-3695-2015>
- Lee, X., Massman, W., & Law, B. (2004). *Handbook of micrometeorology: A guide for surface flux measurement and analysis*. Dordrecht, The Netherlands: Kluwer.
- Liu, H., Blanken, P. D., Weidinger, T., Nordbo, A., & Vesala, T. (2011). Variability in cold front activities modulating cool-season evaporation from a southern inland water in the USA. *Environmental Research Letters*, 6(2), 024022. <https://doi.org/10.1088/1748-9326/6/2/024022>
- Liu, H., Zhang, Q., Katul, G. G., Cole, J. J., Chapin, F. S. III, & MacIntyre, S. (2016). Large CO<sub>2</sub> effluxes at night and during synoptic weather events significantly contribute to CO<sub>2</sub> emissions from a reservoir. *Environmental Research Letters*, 11(6), 064001. <https://doi.org/10.1088/1748-9326/11/6/064001>

- Loken, L., Crawford, J. T., Schramm, P. J., Stadler, P., Desai, A. R., & Stanley, E. H. (2019). Large spatial and temporal variability of carbon dioxide and methane in a eutrophic lake. *Journal of Geophysical Research: Biogeosciences*, *124*, 2248–2266. <https://doi.org/10.1029/2019JG005186>
- Loken, L., Stanley, E., Schramm, P., & Gahler, M. (2019). Spatial surface water chemistry of Lake Mendota with FLAME: 2014–2016.
- López Bellido, J., Tulonen, T., Kankaala, P., & Ojala, A. (2009). CO<sub>2</sub> and CH<sub>4</sub> fluxes during spring and autumn mixing periods in a boreal lake (Pääjärvi, southern Finland). *Journal of Geophysical Research*, *114*, G04007. <https://doi.org/10.1029/2009JG000923>
- Maberly, S. (1996). Diel, episodic and seasonal changes in pH and concentrations of inorganic carbon in a productive lake. *Freshwater Biology*, *35*(3), 579–598. <https://doi.org/10.1111/j.1365-2427.1996.tb01770.x>
- Maberly, S., Barker, P. A., Stott, A. W., & De Ville, M. M. (2012). Catchment productivity controls CO<sub>2</sub> emissions from lakes. *Nature Climate Change*, *3*(4), 391–394.
- MacIntyre, S., Jonsson, A., Jansson, M., Aberg, J., Turney, D. E., & Miller, S. D. (2010). Buoyancy flux, turbulence, and the gas transfer coefficient in a stratified lake. *Geophysical Research Letters*, *37*, L24604. <https://doi.org/10.1029/2010GL044164>
- Magnuson, J., Carpenter, S., & Stanley, E. (2019). North temperate lakes LTER: High frequency water temperature data-lake Mendota buoy 2006-current.
- Mammarella, I., Nordbo, A., Rannik, Ü., Haapanala, S., Levula, J., Laakso, H., et al. (2015). Carbon dioxide and energy fluxes over a small boreal lake in Southern Finland. *Journal of Geophysical Research: Biogeosciences*, *120*, 1296–1314. <https://doi.org/10.1002/2014JG002873>
- Martinsen, K. T., Kragh, T., & Sand-Jensen, K. (2018). Technical note: A simple and cost-efficient automated floating chamber for continuous measurements of carbon dioxide gas flux on lakes. *Biogeosciences*, *15*(18), 5565–5573. <https://doi.org/10.5194/bg-15-5565-2018>
- Mauder, M., & Foken, T. (2015). Documentation and instruction manual of the eddy-covariance software package TK3 (update), Univ., Abt. Mikrometeorologie.
- Moffat, A. M., Papale, D., Reichstein, M., Hollinger, D. Y., Richardson, A. D., Barr, A. G., et al. (2007). Comprehensive comparison of gap-filling techniques for eddy covariance net carbon fluxes. *Agricultural and Forest Meteorology*, *147*(3–4), 209–232. <https://doi.org/10.1016/j.agrformet.2007.08.011>
- Morin, T., Rey-Sánchez, A., Vogel, C., Matheny, A., Kenny, W., & Bohrer, G. (2018). Carbon dioxide emissions from an oligotrophic temperate lake: An eddy covariance approach. *Ecological Engineering*, *114*, 25–33. <https://doi.org/10.1016/j.ecoleng.2017.05.005>
- Natchimuthu, S., Sundgren, I., Gålfalk, M., Klemetsson, L., Crill, P., Danielsson, Å., & Bastviken, D. (2016). Spatio-temporal variability of lake CH<sub>4</sub> fluxes and its influence on annual whole lake emission estimates. *Limnology and Oceanography*, *61*(S1), S13–S26. <https://doi.org/10.1002/lno.10222>
- Ouyang, Z., Shao, C., Chu, H., Becker, R., Bridgeman, T., Stepien, C., et al. (2017). The effect of algal blooms on carbon emissions in western Lake Erie: An integration of remote sensing and eddy covariance measurements. *Remote Sensing*, *9*(1), 44. <https://doi.org/10.3390/rs9010044>
- Paranaíba, J. R., Barros, N., Mendonça, R., Linkhorst, A., Isidorova, A., Roland, F., et al. (2018). Spatially resolved measurements of CO<sub>2</sub> and CH<sub>4</sub> concentration and gas-exchange velocity highly influence carbon-emission estimates of reservoirs. *Environmental Science & Technology*, *52*(2), 607–615. <https://doi.org/10.1021/acs.est.7b05138>
- Plummer, L. N., & Busenberg, E. (1982). The solubilities of calcite, aragonite and vaterite in CO<sub>2</sub>-H<sub>2</sub>O solutions between 0°C and 90°C, and an evaluation of the aqueous model for the system CaCO<sub>3</sub>-CO<sub>2</sub>-H<sub>2</sub>O. *Geochimica et Cosmochimica Acta*, *46*(6), 1011–1040. [https://doi.org/10.1016/0016-7037\(82\)90056-4](https://doi.org/10.1016/0016-7037(82)90056-4)
- Podgrajsek, E., Sahlée, E., Bastviken, D., Natchimuthu, S., Kljun, N., Chmiel, H., et al. (2016). Methane fluxes from a small boreal lake measured with the eddy covariance method. *Limnology and Oceanography*, *61*(S1), S41–S50. <https://doi.org/10.1002/lno.10245>
- Podgrajsek, E., Sahlée, E., & Rutgersson, A. (2014). Diurnal cycle of lake methane flux. *Journal of Geophysical Research: Biogeosciences*, *119*, 236–248. <https://doi.org/10.1002/2013JG002327>
- Raymond, P. A., Hartmann, J., Lauerwald, R., Sobek, S., McDonald, C., Hoover, M., et al. (2013). Global carbon dioxide emissions from inland waters. *Nature*, *503*(7476), 355–359. <https://doi.org/10.1038/nature12760>
- Read, J. S., Hamilton, D. P., Desai, A. R., Rose, K. C., MacIntyre, S., Lenters, J. D., et al. (2012). Lake-size dependency of wind shear and convection as controls on gas exchange. *Geophysical Research Letters*, *39*, L09405. <https://doi.org/10.1029/2012GL051886>
- Reed, D. E., Dugan, H. A., Flannery, A. L., & Desai, A. R. (2018). Carbon sink and source dynamics of a eutrophic deep lake using multiple flux observations over multiple years. *Limnology and Oceanography Letters*, *3*(3), 285–292. <https://doi.org/10.1002/lol2.10075>
- Reichstein, M., Falge, E., Baldocchi, D., Papale, D., Aubinet, M., Berbigier, P., et al. (2005). On the separation of net ecosystem exchange into assimilation and ecosystem respiration: Review and improved algorithm. *Global Change Biology*, *11*(9), 1424–1439. <https://doi.org/10.1111/j.1365-2486.2005.001002.x>
- Salesky, S. T., Chamecki, M., & Dias, N. L. (2012). Estimating the random error in eddy-covariance based fluxes and other turbulence statistics: The filtering method. *Boundary-Layer Meteorology*, *144*(1), 113–135. <https://doi.org/10.1007/s10546-012-9710-0>
- Schubert, C. J., Diem, T., & Eugster, W. (2012). Methane emissions from a small wind shielded lake determined by eddy covariance, flux chambers, anchored funnels, and boundary model calculations: a comparison. *Environmental Science & Technology*, *46*(8), 4515–4522. <https://doi.org/10.1021/es203465x>
- Shao, C., Chen, J., Stepien, C. A., Chu, H., Ouyang, Z., Bridgeman, T. B., et al. (2015). Diurnal to annual changes in latent, sensible heat, and CO<sub>2</sub> fluxes over a Laurentian Great Lake: A case study in Western Lake Erie. *Journal of Geophysical Research: Biogeosciences*, *120*, 1587–1604. <https://doi.org/10.1002/2015JG003025>
- Tangen, B. A., Finocchiaro, R. G., Gleason, R. A., & Dahl, C. F. (2016). Greenhouse gas fluxes of a shallow lake in south-central north Dakota, USA. *Wetlands*, *36*(4), 779–787. <https://doi.org/10.1007/s13157-016-0782-3>
- Tranvik, L. J., Downing, J. A., Cotner, J. B., Loiselle, S. A., Striegl, R. G., Ballatore, T. J., et al. (2009). Lakes and reservoirs as regulators of carbon cycling and climate. *Limnology and Oceanography*, *54*(6part2), 2298–2314.
- Vachon, D., Prairie, Y. T., & Cole, J. J. (2010). The relationship between near-surface turbulence and gas transfer velocity in freshwater systems and its implications for floating chamber measurements of gas exchange. *Limnology and Oceanography*, *55*(4), 1723–1732. <https://doi.org/10.4319/lno.2010.55.4.1723>
- Vachon, D., Prairie, Y. T., & Smith, R. (2013). The ecosystem size and shape dependence of gas transfer velocity versus wind speed relationships in lakes. *Canadian Journal of Fisheries and Aquatic Sciences*, *70*(12), 1757–1764. <https://doi.org/10.1139/cjfas-2013-0241>
- Vesala, T., Eugster, W., & Ojala, A. (2012). Eddy covariance measurements over lakes. In *Eddy covariance*, edited (pp. 365–376). New York: Springer.
- Weyhenmeyer, G. A., Kortelainen, P., Sobek, S., Müller, R., & Rantakari, M. (2012). Carbon dioxide in boreal surface waters: A comparison of lakes and streams. *Ecosystems*, *15*(8), 1295–1307. <https://doi.org/10.1007/s10021-012-9585-4>

- Wik, M., Thornton, B. F., Bastviken, D., Uhlbäck, J., & Crill, P. M. (2016). Biased sampling of methane release from northern lakes: A problem for extrapolation. *Geophysical Research Letters*, *43*, 1256–1262. <https://doi.org/10.1002/2015GL066501>
- Williamson, C. E., Saros, J. E., Vincent, W. F., & Smol, J. P. (2009). Lakes and reservoirs as sentinels, integrators, and regulators of climate change. *Limnology and Oceanography*, *54*(6part2), 2273–2282.
- Xu, K., Pinguha-Durden, N., Luo, H., Durden, D., Sturtevant, C., Desai, A. R., et al. (2019). The eddy-covariance storage term in air: Consistent community resources improve flux measurement reliability. *Agricultural and Forest Meteorology*, *279*, 107734. <https://doi.org/10.1016/j.agrformet.2019.107734>